Ca2+-based metal-organic framework as enzyme preparation to promote the catalytic activity of amylase

J. Song, X. Shen, F. Liu, X. Zhao, Y. Wang, S. Wang, P. Wang, J. Wang, F. Su, S. Li

Ca^{2+} based metal-organic framework as enzyme preparation to promote the catalytic activity of amylase

Jie Song,[a,b] Xin Shen,[a,b] Fangyu Liu,[a,b] Xinshuang Zhao,[a,b] Yuandou Wang, [a,b] Shuxin Wang,[a,b] Pinyi Wang,[c] Jinjun Wang,[c] Feng Su,[a,b*] Suming Li [d*]*

[a] *State Key Laboratory Base of Eco-chemical Engineering, College of Chemical Engineering, Qingdao University of Science and Technology, Qingdao 266042, China*

[b] *Institute of High Performance Polymers, Qingdao University of Science and Technology, Qingdao 266042, China*

[c] *Qingdao Traditional Chinese Medicine Hospital (Qingdao Hiser Hospital), Qingdao 266033, China*

[d] *Institut Europeen des Membranes, IEM, UMR 5635, Univ Montpellier, CNRS, ENSCM, 34095 Montpellier, France*

*Corresponding authors: yayang2001@163.com (J. Wang); sufeng@qust.edu.cn (F. Su); suming.li@umontpellier.fr (S. Li)

Abstract

Enzyme preparation can protect the enzyme conformation in storage, transportation, and operation process, but excessive additives can affect enzyme performance. In this work, a Ca^{2+} based metal-organic framework (UTSA-280) was prepared to encapsulate amylases (α-amylase, pullulanase, and glucoamylase) in situ. After release from UTSA-280, the relative activity of α-amylase and pullulanase increased to 177.8 and 201.0 %, respectively, as compared to pure enzymes. Mechanism explorations indicate that amylase released from UTSA-280 has more Ca^{2+} on its surface with stronger combination, which probably leads to the activation effect to metal ion activating enzyme. Besides, UTSA-280 could protect enzymes from heat, organic solvent, and trypsin, which is beneficial for the storage, transportation, and operation of enzyme. Therefore, it is concluded that MOFs could be a promising metal ion activating enzyme preparation material with activity promoting and protective effects.

Keywords: Metal-organic frameworks; enzyme preparation; amylase; catalysis.

1. Introduction

Traditional enzyme preparations usually suffer from a number of disadvantages such as excessive additives, redundant purification operations, and reduced activity, which could restrain their application [1, 2]. Enzyme preparations often possess a small portion of active enzyme molecules, while a large amount of additives such as inactive proteins, preservatives, salts, and polymers are added to maintain the enzyme conformation on storage conditions [3-6]. However, excessive additives could affect the enzyme performance [7]. On the other hand, addition of enzyme activators such as metal ions is often ineffective and costly because high concentrations of activators are needed due to their low accessibility to and weak interactions with enzyme molecules in the catalytic process [8]. For example, a large amount of ammonium sulfate usually used in the salting-out process, as well as high operating temperature of spray drying, can significantly affect the enzyme performance [9]. Therefore, it is of crucial importance to develop advanced materials for uses in enzyme preparation.

In enzyme applications, metal ions (Mn^{2+}, Zn^{2+}, Ca^{2+}, $Fe^{2+/3+}$) are often required to monitor the activity of enzymes [10]. For example, Ca^{2+} ions are considered to have crucial roles for maintaining α-amylase structures in their correct conformations and improving the thermal resistance [11-13]. Mao and Kinsella found that banana α-amylase activity increased significantly when calcium was incorporated into the assay medium [14]. Mg^{2+} and K^{+} are typical activators of methionine adenosyltransferase (MAT) from all sources which can enhance its activity and reaction rate [15]. Therefore, metal ions are excellent stabilizer and activator of enzymes, and incorporating metal ions as a component is a promising approach for metal ion activating enzyme preparations.

Metal-organic frameworks (MOFs) are an emerging class of crystalline materials assembled by organic links and metal ions or clusters. Owing to their unique properties such as high surface areas, ultra high porosity, high thermal stability, and good surface chemistry,

MOFs have become an ideal material for the preparation of enzyme/MOF biocomposites [16]. In fact, MOFs present several advantages for enzyme encapsulation, i.e. mild preparation environments (room temperature, aqueous solution), high loading efficiency and good protection for enzymes [17, 18]. In the past decade, great efforts have been made to develop enzyme@MOF composites for enzyme immobilization. However, these heterogeneous biocatalytic systems suffer from the decrease of enzyme activity caused by the immobilization and diffusion processes. Interestingly, unstable MOFs could degrade under mild conditions, releasing metal ions which could become enzyme activator. Therefore, enzyme-MOF composites could be promising as high-performance enzyme preparations.

Amylases are a class of industrial enzymes representing approximately 30% of the world enzyme production [19]. Amylases are used in many industrial processes such as food, fermentation, paper, sugar and pharmaceutical industries. Calcium ions play an important role in monitoring the structure, activity, and thermal stability of some amylases [11, 12], thus affecting their performance [20, 21]. However, there is no report on the use of Ca^{2+} based MOF for amylase preparation in spite of its potential in activating amylases.

In this study, a Ca^{2+} based MOF, namely UTSA-280, was synthesized as Ca^{2+} activating enzyme preparation for α-amylase and pullulanase as shown in Scheme 1. UTSA-280 could efficiently encapsulate enzymes in-situ under mild synthesis conditions. The release performance of enzyme@UTSA-280 and the activity of released enzymes were evaluated. Mechanism experiments were performed to understand the strong increase in enzyme activity. The enzyme protection performance and size control of enzyme@UTSA-280 were also explored to further evaluate the potential of UTSA-280 as enzyme preparation material.

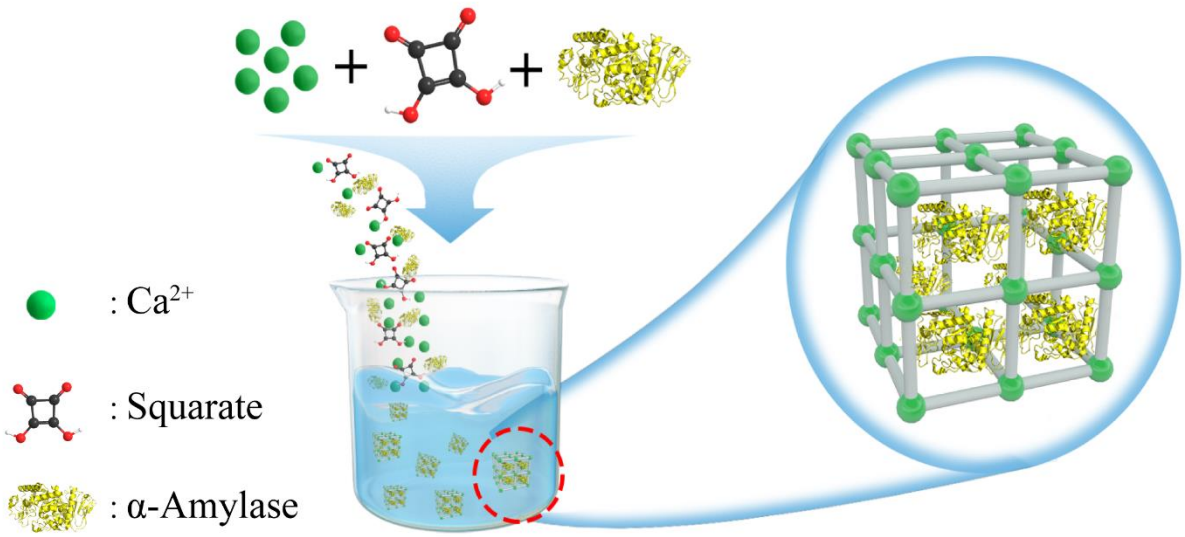

Scheme 1. Schematic description of enzyme@UTSA-280 preparation by in-situ method.

2. Materials and methods

2.1 Materials and reagents

Squaric acid (98%), calcium nitrate tetrahydrate ($Ca(NO_3)_2 \cdot 4H_2O$, 99%), starch (analytical grade) and pullulan (analytical grade) were purchased from Mucklin (Shanghai, China). α-Amylase (from Bacillus subtilis, 4000 U g^{-1}) was obtained from Coolaber (Beijing, China). Glucoamylase (from Aspergillus niger variant strain, >100,000 U g^{-1}) was purchased from Meilunbio (Dalian, China). Pullulanase (from Klebsiella, >1000 U g^{-1}) was obtained from Mucklin (Shanghai, China). Citric acid (≥99.5%), sodium citrate dihydrate (99%), fluorescein isothiocyanate (FITC, ≥90%), HEPES buffer solution (pH 7.0), MES monohydrate (99%), polyvinylpyrrolidone (PVP, MW: 10 kDa) were supplied by Mucklin (Shanghai, China). All enzymes were further purified before use (Supplementary data). All solvents were of analytical grade and used as received.

2.2 Synthesis of materials

2.2.1 Synthesis of UTSA-280

UTSA-280 was synthesized as follows. Aqueous solutions of $Ca(NO_3)_2 \cdot 4H_2O$ (2 mL, 26 mg mL^{-1}) and sodium squarate (2 mL, 15 mg mL^{-1}) were mixed under stirring. The reaction then proceeded for 1 h at room temperature. The resulted white crystals were washed 3 times with water, and collected by centrifugation.

2.2.2 Synthesis of enzyme@UTSA-280

Enzyme@UTSA-280 was prepared by using in situ method. A solution of $Ca(NO_3)_2 \cdot 4H_2O$ (2 mL, 26 mg mL^{-1}) was mixed with a solution of sodium squarate (2 mL, 15 mg mL^{-1}) containing enzymes at various concentrations, and reaction proceeded for 1 h at room temperature. The resulted enzyme@UTSA-280 crystals were washed 3 times with water, and collected by centrifugation.

2.3 Calculation of encapsulation efficiency and loading content

The encapsulation efficiency and loading content of enzymes was determined via standard Bradford assay. Typically, the enzyme encapsulation efficiency of the preparations was calculated via determining the enzyme concentration of the supernatant solution before and after encapsulation by Bradford assay. The encapsulation efficiency and loading content were calculated from the following formulae:

$$\text{Encapsulation efficiency } \% = \frac{C_0 - Cs}{C_0} \times 100\% \quad (1)$$

Where C_0 is the initial enzyme concentration before encapsulation, and C_s is the enzyme concentration of supernatant after encapsulation.

$$\text{Loading content } (mg\ mg^{-1}) = \frac{W_0 - W_s}{W_M - (W_0 - W_s)} \quad (2)$$

Where W_0 is the weight of enzyme before encapsulation, W_s is the enzyme weight in supernatant after encapsulation, and W_M is the weight of enzyme@UTSA-280.

122

123 *2.4 Characterization*

124 X-ray diffraction (XRD) patterns were recorded in the 2θ range from 5 to 50° on a Rigaku
125 d_{max} 2500 diffractometer using Cu Kα (λ = 1.5418 Å) radiation, with a scan speed of 1 sec/step,
126 and a step size of 0.02°. Fourier transform infrared (FT-IR) spectra were registered using a
127 Thermo Fisher spectrometer in ATR mode. 128 scans were made for each measurement in the
128 wavenumber range from 500 to 4000 cm^{-1} at a resolution of 2 cm^{-1}. Circular dichroism (CD)
129 measurements were performed using a spectropolarimeter BioLogic MOS-450. The spectra
130 were collected at a rate of 60 nm per minute and a response time of 16 s. Scanning electron
131 microscopy (SEM) was realized using JSM-7610F filed-emission microscope. Freeze-dried
132 crystals were gold-coated for 90 s and observed using an electron beam at accelerating voltage
133 of 10.0 kV.

134

135 *2.5* Activity test of α-amylase

136 The activity of α-amylase was determined according to the 3, 5-dinitrosalicylic acid
137 (DNS) method [12]. 2 mg of α-amylase@UTSA-280 was placed in 1 mL of citrate buffer (50
138 mM, pH 6.0), and released α-amylase was determined by using Bradford method. The
139 concentration of original and released α-amylase was adjusted to 0.1 mg mL^{-1}. 50 μL of original
140 α-amylase or released α-amylase (50 μg mL^{-1}) were added in 5 mL of HEPES buffer (50 mM,
141 pH 7.0) containing 1.0 wt% soluble starch. The relative activity (%) was the ratio between the
142 activities of released and original α-amylases. All measurements were repeated three times.
143 The activity of pullulanase and glucoamylase was determined using the same method, and the
144 detailed steps are described in Supplementary data.

145

146 *2.6* Enzymatic kinetic parameters determination

147 Enzymatic kinetic parameters were determined according to the literature [22]. The
148 kinetic constants (V_{max}, K_m, K_{cat}) were derived from Lineweaver Burke plot by using eq. 3 and
149 eq. 4.

$$1/V = (K_m/V_{max}) * 1/[S] + 1/V_{max} \quad (3)$$

$$K_{cat} = V_{max}/[e] \quad (4)$$

150 Where [S] is the substrate concentration, and [e] is the molar concentration of α-amylase.
151 To determine the kinetic parameters of released and pure α-amylase, experiments were
152 performed at 37 ℃ with different concentrations of soluble starch of 0.1 to 2.0 wt% in HEPES
153 buffer solution (pH 7.0), at an initial enzyme concentration of 10 μg mL^{-1} and a reaction time
154 of 1 min. The amount of produced glucose was determined by DNS method.
155
156 *2.7* Enzyme protection assay
157 Pure α-amylase powder (10 mg) and α-amylase@UTSA-280 composite (10 mg) were
158 treated by exposure to heat (80 ℃), trypsin solution (1 mg mL^{-1}), and acetone for 1 h. After
159 treatment, α-amylase was released from UTSA-280 in citrate buffer (pH 6.0), and the enzyme
160 concentration was determined by using Bradford method. Then, the activity of pure and
161 released α-amylases was measured by using DNS method and compared to untreated enzymes.
162
163 **3. Results and discussion**
164 *3.1 Characterization of UTSA-280*
165 UTSA-280 was synthesized by reaction between calcium nitrate hexahydrate and sodium
166 squarate under mild conditions in water [23]. Sodium squarate was previously obtained by
167 neutralization of squaric acid using NaOH, as shown in Supplementary data [24]. In as-
168 synthesized UTSA-280, the Ca atom (pentagonal bipyramidal) is coordinated by seven O atoms
169 from five squarate linkers and one water molecule, resulting in one-dimensional channels (Fig.

1a). The hydrogen bonding between coordinated H_2O molecules and O atoms of squarate linkers could further stabilize the framework by restrain the rotation of the organic linkers (Fig. 1b). The XRD pattern of UTSA-280 exhibits high crystallinity in comparison with the calculated pattern, as shown in Fig. 1c. The FT-IR spectrum of UTSA-280 shows various characteristic signals (Fig. 1d), especially those at 1088, 1450, and 3231 cm^{-1}, corresponding to C-O, C=C, and O-H bonds, respectively. TGA data reveal the good thermal stability of UTSA-280 (Fig. 1e). A weight loss of 7.2 % is observed from 50 to 96 ℃, corresponding to the loss of H_2O molecules in the channels. Weight loss of 10.2 % between 156 to 303 ℃ corresponds to the loss of H_2O coordinated with Ca^{2+} ions. Weight loss beyond 392 ℃ results from the framework decomposition. UTSA-280 exhibits a cylindrical crystal structure as shown in Fig. 1f, in agreement with high crystallinity. All these data demonstrate the successful synthesis of uniform UTSA-280 crystals.

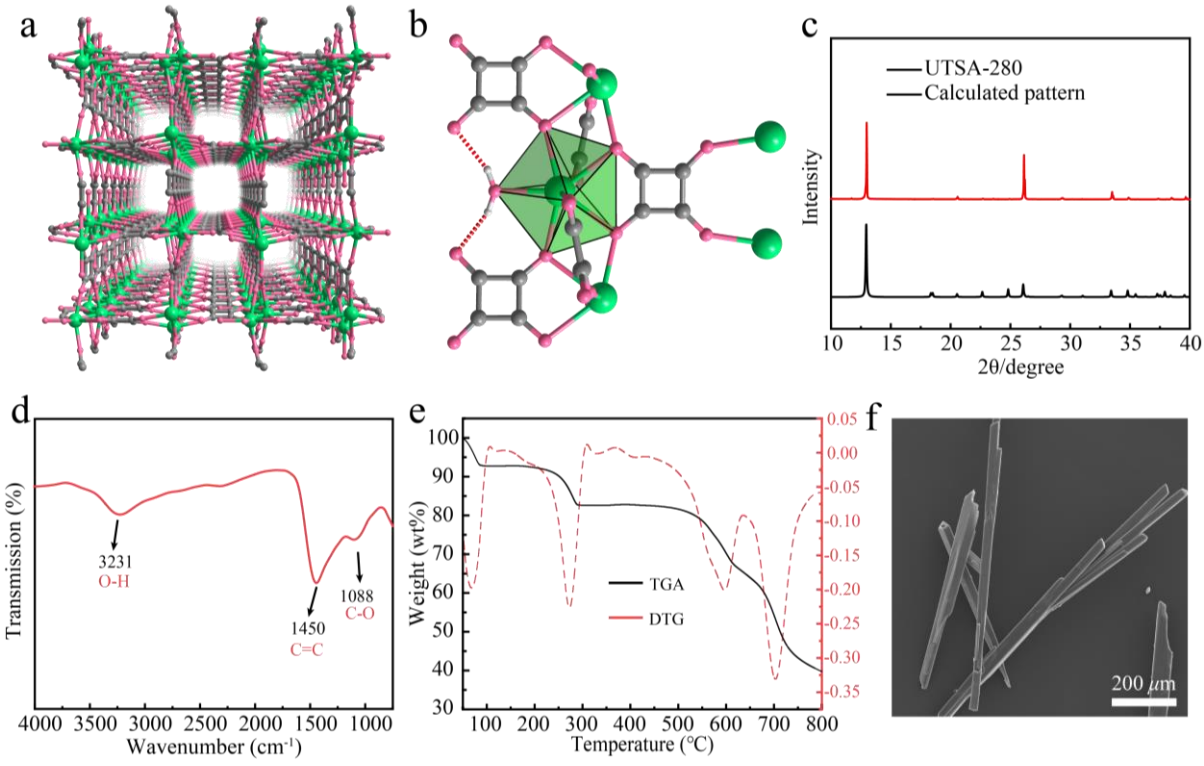

Fig. 1 Structure and characterization of UTSA-280: (a) Crystal structure of UTSA-280, showing one-dimensional channels viewed along the [001] direction. Green, red, and grey balls

represent Ca, O and C atoms, respectively. (b) Local coordination environment of the squarate linkers and Ca atoms. (c) XRD pattern of UTSA-280. (d) Infrared spectrum of UTSA-280. (e) TGA and DTG patterns of UTSA-280. (f) SEM image of UTSA-280.

3.2 Characterization of α-amylase@UTSA-280

α-amylase@UTSA-280 was synthesized in-situ under mild conditions. In this reaction, α-amylase is added together with metal ions and ligand, and α-amylase is loaded during the crystallization process of MOFs. Bradford method was employed to determine the enzyme concentration in α-amylase@UTSA-280. A calibration curve was first established using α-amylase as the standard. A good linearity was obtained from the regression line in the 0.1-1.5 mg mL^{-1} range (Fig. 2a). The encapsulation efficiency and loading content of α-amylase@UTSA-280 were then calculated (Fig. 2b-c). With increasing the initial enzyme concentration from 1.0 to 5.0 mg mL^{-1}, the encapsulation efficiency decreases from 61% to 38%, and the loading content increases from 0.036 to 0.109 mg mg^{-1}. α-Amylase@UTSA-280 at enzyme concentration of 2 mg mL^{-1} was selected for subsequent experiments as it has suitable encapsulation efficiency (59.2 ± 1.0 %) and loading content (0.070 ± 0.004 mg mg^{-1}).

Fig. 2d shows the XRD patterns of α-amylase@UTSA-280 and UTSA-280. Both present the same diffraction peaks, indicating that enzyme encapsulation didn't affect the crystalline structure and crystallinity of UTSA-280, even at an enzyme concentration of 5 mg mL^{-1} in the synthesis process (Fig. S1). In the FT-IR spectra (Fig. 2e), a band assigned to the bending vibration of the N–H group is detected at 1646 cm^{-1} for α-amylase and α-amylase@UTSA-280, but not for UTSA-280, thus demonstrating the successful synthesis of α-amylase@UTSA-280. The thermal stability of α-amylase@UTSA-280 was evaluated by TGA under nitrogen atmosphere in comparison with α-amylase (Fig. 2f). In the TGA thermogram of α-amylase@UTSA-280, a weight loss of 6.9 % is observed from 50 to 96 °C, corresponding to

the loss of H_2O molecules. Weight loss of 9.9% between 168 to 287 ℃ belongs to α-amylase decomposition and the loss of H_2O coordinated with Ca ions in UTSA-280. Weight loss beyond 430 ℃ mainly results from the MOF framework. In contrast, an almost continuous weight loss is observed for α-amylase beyond 200°C due to its decomposition. In SEM image of α-amylase@UTSA-280 (Fig. 2g), rod-like aggregates of crystals are observed. α-Amylase was labeled by FITC (Supplementary data). Confocal laser scanning microscopy (CLSM) shows a uniform distribution of FITC-labeled α-amylase in UTSA-280 (Fig. 2h). All these data prove that α-amylase is successfully encapsulated in UTSA-280.

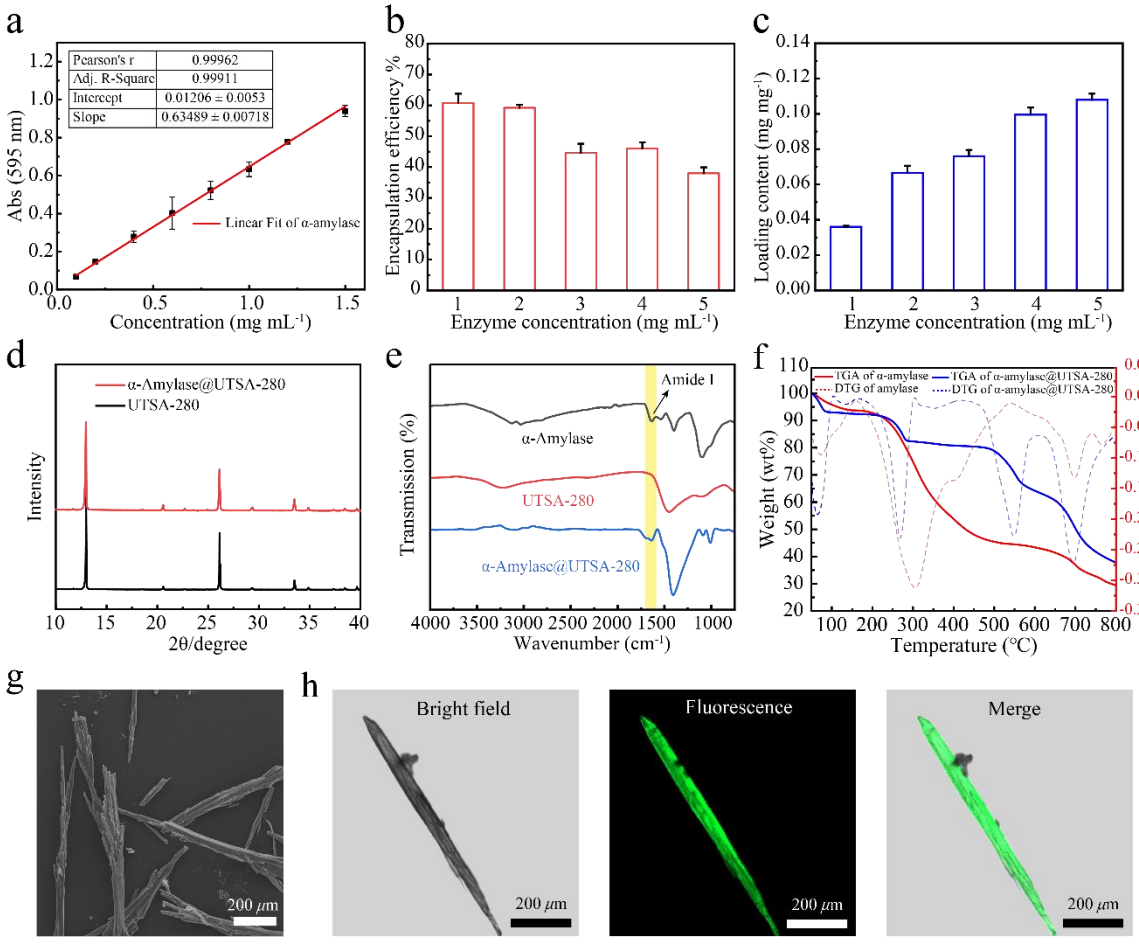

Fig. 2. Characterization of α-amylase@UTSA-280: (a) linear fitting of α-amylase by Bradford method; (b-c) the encapsulation efficiency and loading content of α-amylase@UTSA-280; (d) XRD patterns of UTSA-280 and α-amylase@UTSA-280; (e) FT-IR spectra of α-amylase, UTSA-280, and α-amylase@UTSA-280; (f) TGA and DTG patterns of α-amylase and α-

amylase@UTSA-280; (g) SEM image of α-amylase@UTSA-280; (h) CLSM images α-amylase@UTSA-280.

3.3 Enzyme release behavior of α-amylase@UTSA-280

The absorbance of α-amylase was determined at 540 nm in MES buffers at various pH in order to determine the suitable releasing pH value. As shown in Fig. 3a, α-amylase exhibits high activity between pH 5.0-7.0. Therefore, the enzyme release behavior from α-amylase@UTSA-280 was evaluated in this pH range (Fig. 3b). Biphasic release profiles are observed in all cases with initial faster release followed by slower release. The release rate increases with pH decrease, which could be attributed to the accelerated degradation of MOFs under acidic conditions. The degradability and enzyme loading properties of UTSA-280 make it a potential enzyme preparation material.

Maintaining enzyme conformation during the storage and operation process is crucial for the application of enzymes. Thus, the secondary structure of α-amylase was determined using circular dichroism (CD) to confirm the protective effect of MOFs. Released α-amylase was collected via ultrafiltration with 8 kDa MWCO device to remove impurities (digested ligands and metal salts). Notably, both pristine α-amylase and released α-amylase exhibit a typical α-helix structure without any difference [25], suggesting that the in-situ encapsulation process did not affect the conformation of enzyme (Fig. 3c).

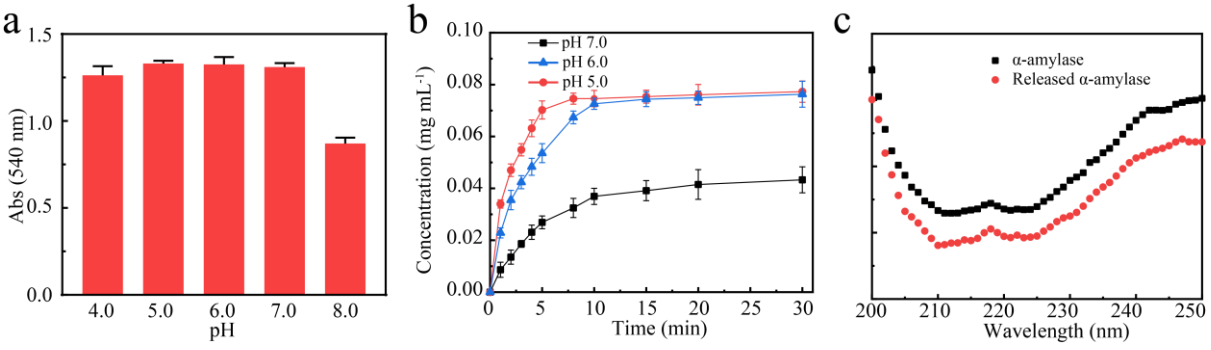

Fig. 3 (a) Absorbance of α-amylase at different pH values; (b) enzyme release profiles in citrate buffer (50 mM, pH 5.0-7.0); (c) CD spectra of pristine α-amylase and α-amylase released from UTSA-280.

3.4 Catalytic activity test

The catalytic activity of released α-amylase was determined using soluble starch as the substrate in HEPES buffer (50 mM, pH 7.0). The concentration of produced glucose was measured using a previously established calibration curve (Fig. S2) [26]. Fig. 4a shows the glucose concentration changes as a function of reaction time in the presence of pristine α-amylase, released α-amylase, α-amylase + $Na_2C_4O_4$, α-amylase + Ca^{2+}, and UTSA-280. The added concentrations of Ca^{2+} and $Na_2C_4O_4$ were 11.75 mM, *i.e.* equal to that of released α-amylase. Higher glucose concentration is obtained for released α-amylase during the whole reaction period up to 20 min. The relative activity of released α-amylase is 177.8% compared to pristine α-amylase. In contrast, direct addition of Ca^{2+} or squaric acid has no effect on the enzyme activity, and pure UTSA-280 material has no catalytic effect. Further investigation suggests that a relatively high concentration (100 mM) of free Ca^{2+} is required to achieve a relative activity of 127.0 % at an incubation enzyme concentration of 2 mg mL^{-1} (Fig. 4c), and the Ca^{2+} concentration during synthesis (79.2 mM) does not have such a promoting effect. Fig. 4d shows that sodium squarate has little influence on the activity of α-amylase. Therefore, the enhanced activity is likely related to the release process. These results suggest that metal ion activators from the enzyme/MOF matrix could strongly ameliorate the enzymatic activity, which might be attributed to the enhanced interactions between calcium ions and enzyme molecules during the release process.

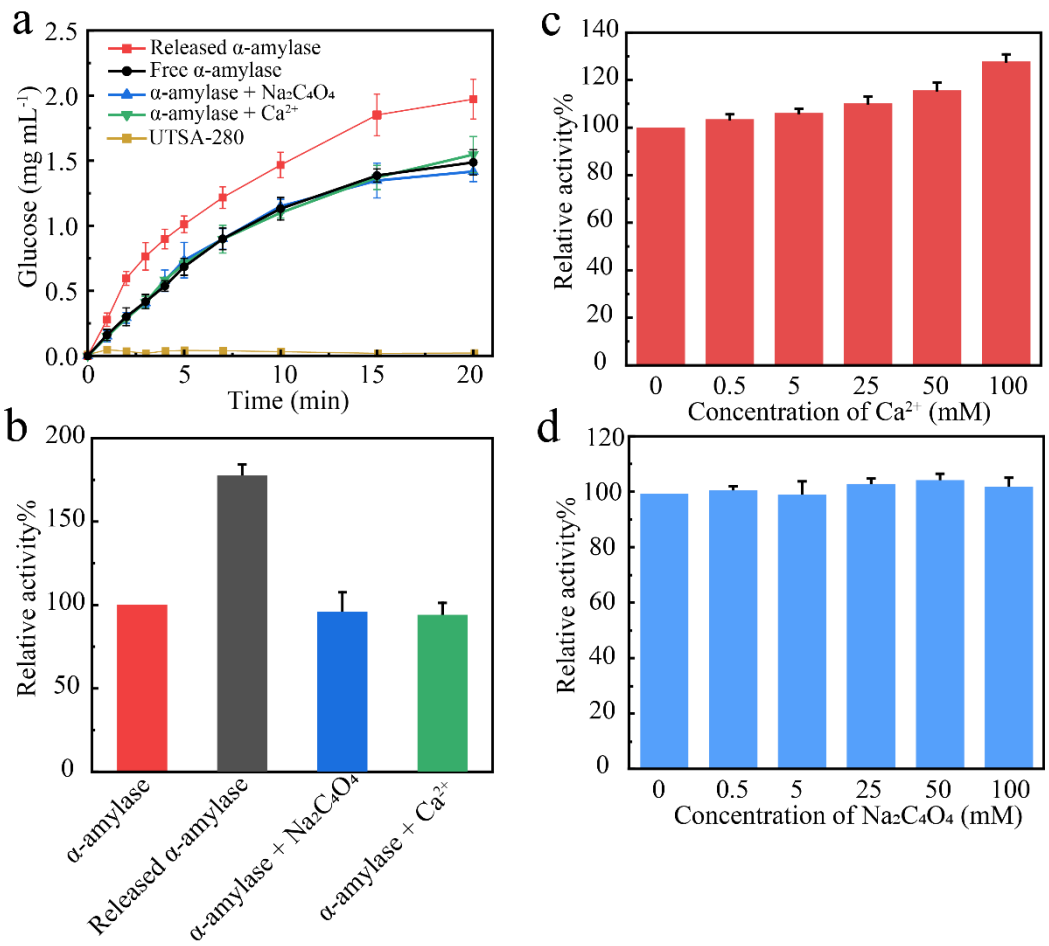

Fig. 4 (a) Glucose concentration changes as a function of reaction time in the presence of pristine α-amylase, released α-amylase, α-amylase + $Na_2C_4O_4$, α-amylase + Ca^{2+}, and UTSA-280; (b) relative activity of α-amylase, released α-amylase, α-amylase + $Na_2C_4O_4$, and α-amylase + Ca^{2+}; (c) relative activity of α-amylase in the presence of Ca^{2+} at different concentrations; (d) relative activity of α-amylase in the presence of $Na_2C_4O_4$ at different concentrations. Test conditions: 1 wt% soluble starch solution in HEPES buffer (50 mM, pH 7.0) at 37 ℃.

3.5 Exploration of mechanism for the increase of enzymatic activity

Energy dispersive X-ray spectroscopy (EDX) was used to characterize the released α-amylase in comparison with purchased one so as to figure out the mechanism for the increase

of enzymatic activity. Released α-amylase and α-amylase incubated with Ca^{2+} were collected via ultrafiltration, 3 times washing with deionized water to remove free Ca^{2+}, and freeze-drying. As shown in Fig. 5a-c and Table 1, released α-amylase has higher Ca^{2+} content (10.7 ±2.3 % of weight, 4.3±1.1 % of atom) than purchased α-amylase (2.8±0.4 % of weight, 0.7 ±0.1 % of atom) and α-amylase incubated with Ca^{2+} (4.7±0.6 % of weight, 1.6±0.2 % of atom). Inductively coupled plasma-optical emission spectrometry (ICP-OES) was also used to quantify the Ca^{2+} content of these three groups, as shown in Fig. S3. The Ca^{2+} content of released α-amylase, pristine α-amylase, and α-amylase incubated with Ca^{2+} are 99.7±3.3, 4.7±1.1, and 29.2±4.7 μg mg^{-1}, respectively. ICP-OES data are consistent with those of EDX, which revealed that MOF encapsulation enhances enzyme activity more effectively than direct addition of metal ions. These results suggest that the improved enzymatic activity could result from more interaction between Ca^{2+} ions and α-amylase. The enzymatic kinetic parameters of α-amylase released from UTSA-280 were determined by using Lineweaver Burke plot (Fig. S4) and Michaelis-Menten model [22, 27]. The results revealed that released α-amylase has a V_{max} of 0.25 mM s^{-1}, K_m of 0.27 mM, and K_{cat} *of* 1.25*10^3 s^{-1}, while untreated α-amylase has V_{max}, K_m and k_{cat} of 0.14 mM s^{-1}, 0.46 mM and 0.69*10^3 s^{-1}, respectively (Table 2). The lower K_m value of released α-amylase implies higher affinity towards substrates while the higher K_{cat} of released α-amylase could be attributed to the activation effect of Ca^{2+} from UTSA-280, which is consistent with literature data [28].

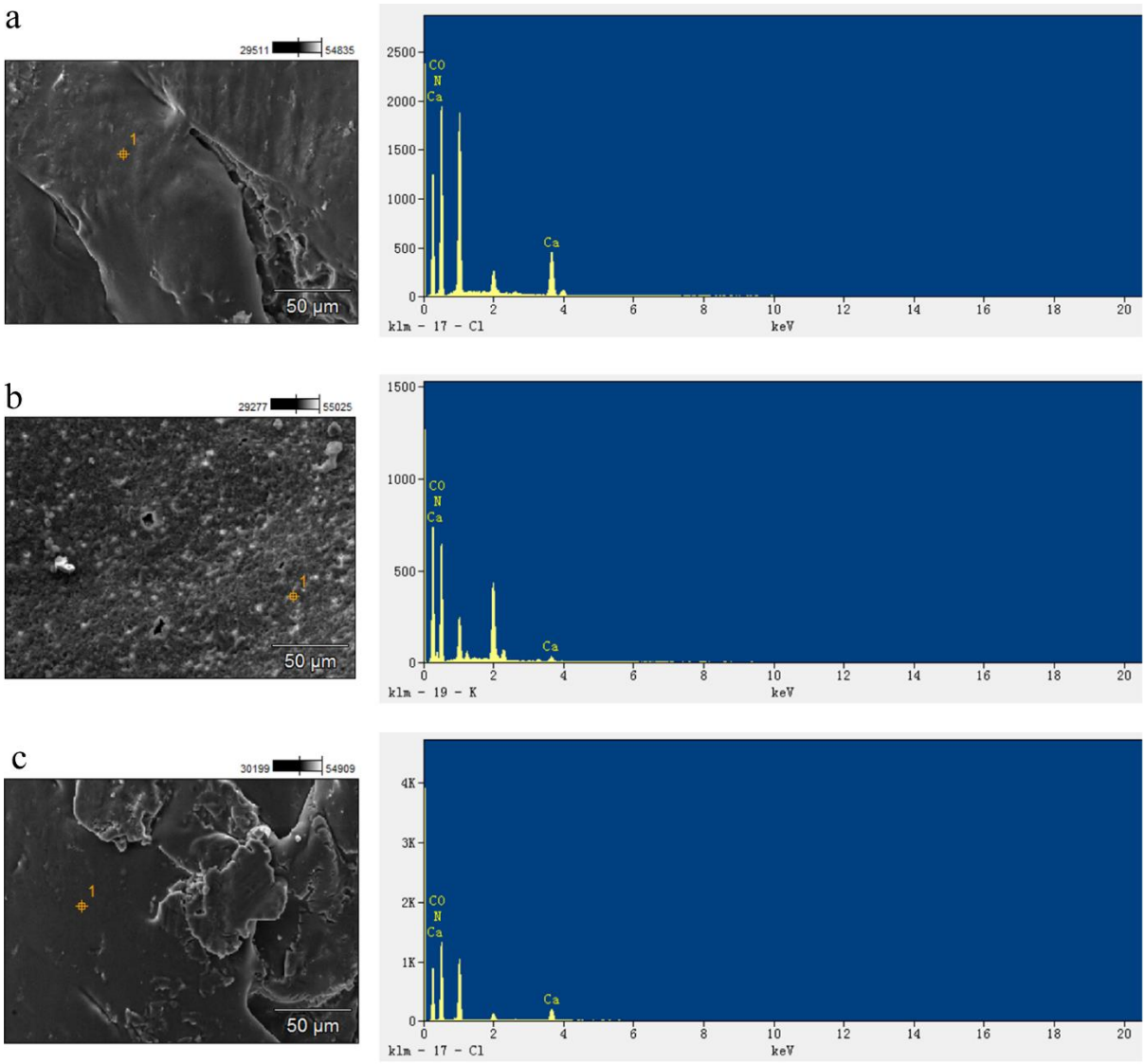

297

298 **Fig. 5.** Energy dispersive X-ray spectroscopy (EDX) of (a) released α-amylase, (b) pristine α-

299 amylase, and (c) α-amylase incubated with Ca^{2+} (11.75 mM) for 1 h. (n=3)

300

301 **Table 1.** Element contents of released α-amylase, pristine α-amylase, and α-amylase incubated

302 with Ca^{2+} (11.75 mM) for 1 h determined by EDX (n=3)

	Element	Weight %	Atom %
Released α-amylase	C	15.8±1.8	20.9±1.9
	O	65.9±0.8	65.9±0.4

Pristine α-amylase	N	7.8±0.2	8.9±0.4
	Ca	10.7±2.3	4.3±1.1
	C	22.3±0.5	29.3±2.1
	O	60.1±3.6	53.0±4.8
α-amylase incubated with Ca^{2+}	N	14.8±0.1	17.3±2.7
	Ca	2.8±0.4	0.7±0.1
	C	12.7±0.5	14.6±3.1
	O	74.2±1.3	72.7±2.1
	N	8.5±1.2	11.2±1.3
	Ca	4.7±0.6	1.6±0.2

Two other enzymes, pullulanase (Ca^{2+} activating enzyme) and glucoamylase (non Ca^{2+} activating enzyme) were also encapsulated in UTSA-280 to better understand the activation effect of UTSA-280. The enzyme concentration was determined by Bradford method using enzyme standard calibration curves (Fig. S5-6). And the encapsulation efficiency and loading content of pullulanase (64.1 ± 2.4%, 0.150 ± 0.011 mg mg^{-1}) and glucoamylase (44.2 ± 3.2%, 0.110 ± 0.004 mg mg^{-1}) were then obtained (Fig. S7). FT-IR spectra and CLSM data prove the successful encapsulation of the two enzymes in UTSA-280 (Fig. S8-10). In addition, XRD and SEM data demonstrate the high crystallinity of UTSA-280 after enzyme encapsulation (Fig. S11-12). Then, pullulanase and glucoamylase were released from UTSA-280 and their catalytic activity was evaluated in the pH range from pH 4.0 to 8.0 (Fig. S13-14). As shown in Fig. S15, the activity of released pullulanase shows a dramatic increase (201 ± 28 %), which may be attributed to the fact that pullulanase is a Ca^{2+} activated enzyme. Meanwhile, glucoamylase, which is not a Ca^{2+} activated enzyme, shows no activity increase. These findings prove that

this strategy can be applied to other Ca^{2+} activated amylases, suggesting that MOFs could serve as metal ion activated enzyme preparation. Thus MOFs materials with different metal ions can be selected according to metal ions-activated enzymes.

Table 2 Kinetic parameters for released α-amylase and pristine α-amylase.

	V_{max} [mM s^{-1}]	K_m [mM]	K_{cat} [10^3 s^{-1}]
Released α-amylase	0.25	0.27	1.25
Pristine α-amylase	0.14	0.46	0.69

3.6 Size control of UTSA-280

The size control of MOFs is important as it affects the release performance of enzymes. Polyvinylpyrrolidone (PVP) is a water soluble polymer with low toxicity and high thermal stability [29]. PVP is widely used as a capping agent to prevent colloidal aggregation, thus allowing to control the size of nanoparticles, especially MOFs [30]. The size of UTSA-280 was adjusted by using PVP to further modulate the release performance of α-amylase from UTSA-280. As shown in Fig. 7a-f and Fig. S16, the crystal size of UTSA-280 decreases from above 1000 μm to below 100 μm with increase of PVP concentration from 0.1 to 1.0 mg mL^{-1}. It is also noteworthy that larger crystal size of UTSA-280 leads to higher loading content (Fig. 6g), and thus leading to higher final concentration of released enzyme (Fig. 6h). XRD patterns show that α-amylase@UTSA-280 synthesized using PVP as capping agent presents the same crystalline structure as that synthesized without PVP (Fig. S17).

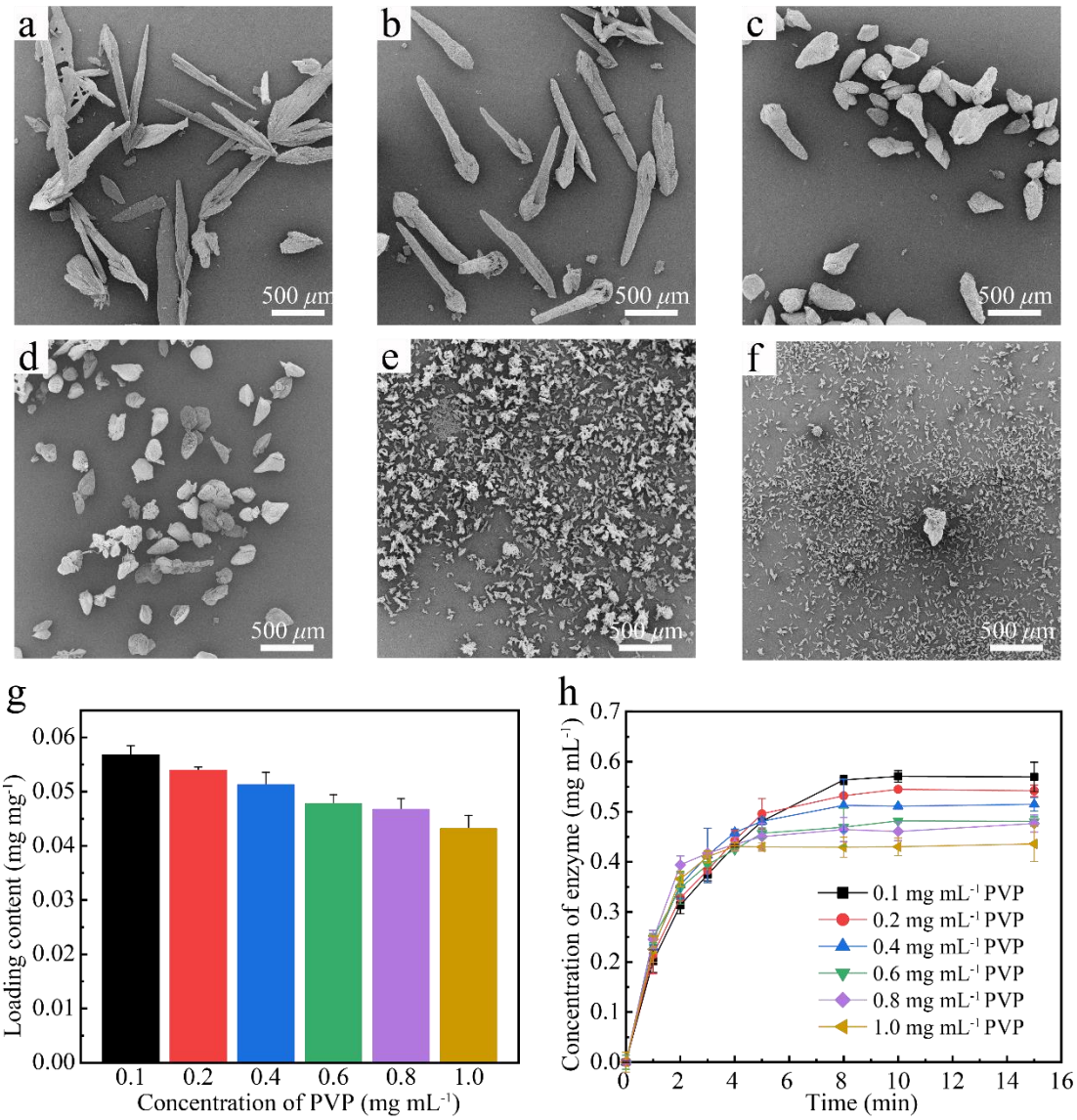

Fig. 6 (a-f) SEM images (30 ×) of, (g) loading content of, and (h) enzyme release profiles from α-amylase@UTSA-280 synthesized using PVP capping agent at concentrations of 0.1, 0.2, 0.4, 0.6, 0.8, 1.0 mg mL^{-1}. Test conditions: 10 mg material in 1 mL citrate buffer (50 mM, pH 6.0) at room temperature.

3.7 Protection assay of α-amylase@UTSA-280

It is of major importance to preserve enzyme activity during the storage and operation process. The confined space created by MOFs should provide excellent protection to enzymes [30]. The protection performance of UTSA-280 to α-amylase was evaluated by exposure to

heat (80 ℃), trypsin (1 mg mL^{-1}), and organic solvent (acetone) for 1 h. As shown in Fig. 7, the relative activity of α-amylase decreases to 67.2, 37.4, and 76.5% after treatment by heat, trypsin, and acetone, respectively. In contrast, the relative activity of enzyme in α-amylase@UTSA-280 is 80.1, 65.6, and 86.4% after the same treatments. These findings indicate that UTSA-280 could efficiently protect α-amylase against harsh conditions. Moreover, sodium squarate presents good biocompatibility according to MTT and live-dead staining experiments. The cell viability is above 81% for all groups (Fig. S18), and no apparent apoptosis is observed (Fig. S19). Therefore, UTSA-280 could facilitate the storage, transport, and operation of enzyme preparations.

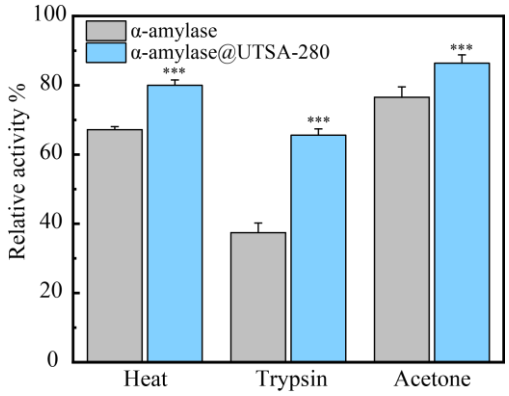

Fig. 7 Relative activity of nude α-amylase and α-amylase@UTSA-280 after 1 h exposure to heat (80 ℃), trypsin (1 mg mL^{-1}), organic solvent (acetone). The enzyme activity was measured in HEPES buffer (50 mM, pH 7.0). (n=3, *** $p<0.001$)

4. Conclusions

MOFs are able to function as metal ion activator and protector, and is thus a material of choice for enzyme preparations, especially metal-activated enzyme preparations. However, there is no research reported on MOFs as a metal ion activated enzyme preparation, so far. In this work, α-amylase and pullulanase were successfully encapsulated in situ in a Ca^{2+} based MOF (UTSA-280) under mild conditions. The enzyme@UTSA-280 composite crystals could

degrade rapidly in acidic environment and release enzyme. Importantly, the structural integrity of released enzyme was preserved as evidenced by CD spectra. The relative activity of released α-amylase and pullulanase increased to 177.8 % and 201.0 % as compared to original enzyme. Mechanistic investigation proves that the increase of enzyme activity could be attributed to the activation by Ca^{2+}. Ca^{2+} could activate α-amylase and pullulanase, but has no effect on glucoamylase which is not Ca^{2+} activated enzyme. Enzyme activity tests after exposure to heat, trypsin, and acetone showed that α-amylase@UTSA-280 provides good protection to enzyme molecules. In addition, the size and enzyme release rate of α-amylase@UTSA-280 can be tailored by using PVP capping agent at different concentrations. Compared with current enzyme preparations, this MOFs based platform present several advantages. Firstly, MOFs could combine the advantages of metal ion activation and enzyme protection, especially for metal ion activating enzymes. Secondly, the preparation conditions are milder than those used in traditional methods such as salting out or spray drying. Thirdly, this platform could avoid the use of excessive additives to maintain the enzyme conformation on storage conditions. Last but not least, this platform can efficiently activate enzymes by providing small amount of activator. Compared to direct addition of activator, this platform is more friendly to applications which require post-processing and purification. Therefore, enzyme@MOFs preparations are most promising for applications in the field of enzyme production, biocatalytic production, and food processing.

Acknowledgments

The work was financially supported by the Shandong Provincial Natural Science Foundation (ZR2020QH271, ZR2021ME208, ZR2022ME083).

Author Contributions

J. Song did most experiments, data analysis, and wrote the manuscript; X. Shen, and F. Liu prepared the specimens and made FT-IR and CD measurements, X. Zhao, Y. Wang, and S. Wang performed kinetic studies of enzymes, P. Wang made FITC-labeling of enzyme; J. Wang, F. Su and S. Li co-initiated the work, and revised the manuscript. All authors discussed and contributed the discussion and analysis of the results regarding the manuscript. All authors have given approval for the final version of the manuscript.

Declaration of competing interest

The authors declare that they have no known competing financial interests or personal relationships that could have appeared to influence the work reported in this paper.

Reference

[1] C. Silva, M. Martins, S. Jing, J. Fu, A. Cavaco-Paulo, Practical insights on enzyme stabilization, Crit. Rev. Biotechnol. 38 (2018), 335-350.

[2] M.A. Singer, S. Lindquist, Multiple effects of trehalose on protein folding in vitro and in vivo, Mol. Cell 1 (1998), 639-648.

[3] S.A. Costa, T. Tzanov, A. Filipa Carneiro, A. Paar, G.M. Gübitz, A. Cavaco-Paulo, Studies of stabilization of native catalase using additives, Enzyme Microb. Technol. 30 (2002), 387-391.

[4] R.V. Parthasarathy, C.R. Martin, Synthesis of polymeric microcapsule arrays and their use for enzyme immobilization, Nature 369 (1994), 298-301.

[5] J.T. Duskey, I. Ottonelli, A. Rinaldi, I. Parmeggiani, B. Zambelli, L.Z. Wang, R.K. Prud'homme, M.A. Vandelli, G. Tosi, B. Ruozi, Tween® preserves enzyme activity and stability in PLGA nanoparticles, Nanomaterials 11 (2021), 2946.

[6] T. Fan, J. Qin, X. Meng, J. Li, Q. Liu, G. Wang, Biodegradable membrane of poly (l-lactide acid-dioxanone-glycolide) and stereocomplex poly (lactide) with enhanced crystallization and biocompatibility, Front. Bioeng. Biotechnol. 10 (2022).

[7] B.t. Limoges, J.-M. Savéant, Catalysis by immobilized redox enzymes. Diagnosis of inactivation and reactivation effects through odd cyclic voltammetric responses, J. Electroanal. Chem. 562 (2004), 43-52.

[8] K.A. Shisler, R.U. Hutcheson, M. Horitani, K.S. Duschene, A.V. Crain, A.S. Byer, E.M. Shepard, A. Rasmussen, J. Yang, W.E. Broderick, J.L. Vey, C.L. Drennan, B.M. Hoffman, J.B. Broderick, Monovalent Cation Activation of the Radical SAM Enzyme Pyruvate Formate-Lyase Activating Enzyme, J. Am. Chem. Soc. 139 (2017), 11803-11813.

[9] S.N. Gummadi, T. Panda, Purification and biochemical properties of microbial pectinases—a review, Process Biochem. 38 (2003), 987-996.

[10] J. He, S. Sun, M. Lu, Q. Yuan, Y. Liu, H. Liang, Metal-nucleobase hybrid nanoparticles for enhancing the activity and stability of metal-activated enzymes, Chem. Commun. 55 (2019), 6293-6296.

[11] N. Goyal, J. Gupta, S. Soni, A novel raw starch digesting thermostable α-amylase from Bacillus sp. I-3 and its use in the direct hydrolysis of raw potato starch, Enzyme Microb. Technol. 37 (2005), 723-734.

[12] S.-M. Liao, G. Liang, J. Zhu, B. Lu, L.-X. Peng, Q.-Y. Wang, Y.-T. Wei, G.-P. Zhou, R.-B. Huang, Influence of calcium ions on the thermal characteristics of α-amylase from thermophilic Anoxybacillus sp. GXS-BL, Protein Pept. Lett. 26 (2019), 148-157.

[13] D.S. Bush, L. Sticher, R. Van Huystee, D. Wagner, R.L. Jones, The calcium requirement for stability and enzymatic activity of two isoforms of barley aleurone α-amylase, J. Biol. Chem. 264 (1989), 19392-19398.

[14] W. Mao, J. Kinsella, Amylase activity in banana fruit: properties and changes in activity with ripening, J. Food Sci. 46 (1981), 1400-1403.

[15] Y. Liu, W. Wang, W. Zhang, Y. Dong, F. Han, M. Raza, L. Liu, T. Tan, Y. Feng, Structure of a thermostable methionine adenosyltransferase from Thermus thermophilus HB27 reveals a novel fold of the flexible loop, RSC adv. 6 (2016), 41743-41750.

[16] C. Doonan, R. Riccò, K. Liang, D. Bradshaw, P. Falcaro, Metal–Organic Frameworks at the Biointerface: Synthetic Strategies and Applications, Acc. Chem. Res. 50 (2017), 1423-1432.

[17] W. Liang, P. Wied, F. Carraro, C.J. Sumby, B. Nidetzky, C.-K. Tsung, P. Falcaro, C.J. Doonan, Metal–Organic Framework-Based Enzyme Biocomposites, Chem. Rev. 121 (2021), 1077-1129.

[18] W. Liang, P. Wied, F. Carraro, C.J. Sumby, B. Nidetzky, C.-K. Tsung, P. Falcaro, C.J. Doonan, Metal–Organic Framework-Based Enzyme Biocomposites, Chemical Reviews 121 (2021), 1077-1129.
[19] M. Mobini-Dehkordi, F.A. Javan, Application of alpha-amylase in biotechnology, J. Biol. Today World 1 (2012), 39-50.
[20] N. Declerck, M. Machius, P. Joyet, G. Wiegand, R. Huber, C. Gaillardin, Hyperthermostabilization of Bacillus licheniformis α-amylase and modulation of its stability over a 50 C temperature range, Protein Eng. 16 (2003), 287-293.
[21] J.W. Torrance, M.W. MacArthur, J.M. Thornton, Evolution of binding sites for zinc and calcium ions playing structural roles, Proteins: Struct., Funct., Bioinf. 71 (2008), 813-830.
[22] F. ADNAN, Kinetics and thermodynamic studies of alpha amylase from Bacillus licheniformis mutant, Pak. J. Bot 42 (2010), 3507-3516.
[23] R.-B. Lin, L. Li, H.-L. Zhou, H. Wu, C. He, S. Li, R. Krishna, J. Li, W. Zhou, B. Chen, Molecular sieving of ethylene from ethane using a rigid metal–organic framework, Nat. Mater. 17 (2018), 1128-1133.
[24] S. Cohen, S.G. Cohen, Preparation and Reactions of Derivatives of Squaric Acid. Alkoxy-, Hydroxy-, and Aminocyclobutenediones1, J. Am. Chem. Soc. 88 (1966), 1533-1536.
[25] T. Konno, Conformational diversity of acid‐denatured cytochrome c studied by a matrix analysis of far‐UV CD spectra, Protein Sci. 7 (1998), 975-982.
[26] G.L. Miller, Use of dinitrosalicylic acid reagent for determination of reducing sugar, Anal. Chem. 31 (1959), 426-428.
[27] L. Michaelis, M.L. Menten, Die kinetik der invertinwirkung, Biochem. z 49 (1913), 352.
[28] H. Torabizadeh, M. Tavakoli, M. Safari, Immobilization of thermostable α-amylase from Bacillus licheniformis by cross-linked enzyme aggregates method using calcium and sodium ions as additives, J. Mol. Catal. B: Enzym. 108 (2014), 13-20.
[29] P. Arul, S.A. John, Size controlled synthesis of Ni-MOF using polyvinylpyrrolidone: New electrode material for the trace level determination of nitrobenzene, J. Electroanal. Chem. 829 (2018), 168-176.
[30] T.-H. Wei, S.-H. Wu, Y.-D. Huang, W.-S. Lo, B.P. Williams, S.-Y. Chen, H.-C. Yang, Y.-S. Hsu, Z.-Y. Lin, X.-H. Chen, Rapid mechanochemical encapsulation of biocatalysts into robust metal–organic frameworks, Nat. Commun. 10 (2019), 1-8.